

Reprint from

Nadia Magnenat-Thalmann  
Daniel Thalmann (Eds.)

## Computer Animation '90

---

Springer-Verlag Tokyo 1990  
Printed in Japan. Not for Sale.



Springer-Verlag  
Tokyo Berlin Heiderberg New York  
London Paris Hong Kong

# Animation of the Development of Multicellular Structures

F. DAVID FRACCHIA, PRZEMYSŁAW PRUSINKIEWICZ, and  
MARTIN J. M. DE BOER

## ABSTRACT

This paper presents a simulation-based method for the animation of the development of cellular layers. The neighborhood relations between the cells are determined using a simulated developmental process, expressed by the formalism of map L-systems. The cell shapes result from mechanical cell interactions. Two types of forces are considered: the osmotic pressure and the tension of cell walls. The animation consists of periods of continuous growth separated by instantaneous cell divisions. The method is illustrated using the fern gametophyte *Microsorium linguaeforme*.

**Keywords:** mathematical modeling in biology, animation through simulation, visualization of development, map L-system, dynamic model.

## 1 INTRODUCTION

An important issue in developmental biology is the study of cell division patterns, that is, the spatial and temporal organization of cell divisions in tissues. This paper presents a method for the visualization of the development of single-layered cellular structures, such as those found in moss leaves and fern gametophytes [de Boer 1989].

The practical motivation for this work is related to two applications. As a *research tool*, graphical simulations make it possible to study the impact of cell divisions on cell arrangement and global shape formation. As a *visualization method*, simulations provide a tool for presenting features that cannot be captured using time-lapse photography. For example, pseudocolor may be introduced to distinguish groups of cells descending from a specific ancestor or to indicate cell age. Inconspicuous structural elements, such as new division walls, can be emphasized.

The underlying mathematical model consists of two components. On a *topological* level, the cell division patterns are expressed using the formalism of *map L-systems*. At this stage the neighborhood relations between cells are established, but the cell shapes remain unspecified. Next, cell *geometry* is modeled using a dynamic method that takes into account the osmotic pressure inside the cells and the tension of cell walls. The animation consists of periods of continuous cell expansion, delimited by cell divisions. The divisions are assumed to be instantaneous.

The paper is organized as follows. Section 2 describes the simulation of cellular development on the topological level. After a brief survey of methods for the parallel generation of graphs with cycles, attention is focused on map L-systems with markers (mBPMOL-systems). Section 3 is devoted to specifying the geometry of cellular structures given their topology. A brief survey of previous methods is given, and a new method, based on the concept of dynamic modeling, is introduced.

The geometry of a cellular structure is viewed as a result of forces acting on cell walls. It changes in time as the entire structure attempts to reach an equilibrium state. Section 4 applies the method to model and visualize the development of a real biological structure — the gametophyte of the fern *Microsorium linguaeforme*. Problems open for future research are outlined in Section 5.

## 2 MAP L-SYSTEMS

### 2.1 Maps as Models of Cell Layers

In order to simulate the development of cell structures, one needs a formalism that will capture the relevant aspects of the developmental process. Cellular layers are represented using a class of planar graphs with cycles, called *maps* [Tutte 1982]. According to Nakamura et al. (1986), maps can be characterized as follows:

- A map is a finite set of *regions*. Each region is surrounded by a boundary consisting of a finite, circular sequence of *edges* which meet at *vertices*.
- Each edge has one or two vertices associated with it.<sup>1</sup> The edges cannot cross without forming a vertex and there are no vertices without an associated edge.
- Every edge is a part of the boundary of a region.
- The set of edges is connected. Specifically, there are no islands within regions.

A map corresponds to a microscopic view of a cellular layer. Regions represent cells, and edges represent cell walls perpendicular to the plane of view. We abstract here from the internal components of a cell.

### 2.2 Rewriting Systems and Cell Layer Development

The process of cell division can be expressed as map rewriting. This notion is an extension of string rewriting used in formal language theory. In general, map rewriting systems are categorized as *sequential* or *parallel*, and can be *region-controlled* or *edge-controlled*. Since several cells may divide concurrently, a parallel rewriting system is needed. The second categorization has to do with the form of rewriting rules, which may express cell subdivisions in terms of region labels or edge labels. Both approaches are suitable for biological modeling purposes [de Boer 1989]. We have chosen an edge-controlled formalism of *Binary Propagating Map OL-system with markers*, or mBPMOL-systems. It was proposed by Nakamura, Lindenmayer and Aizawa (1986) as a refinement of the basic concept of map L-systems introduced by Lindenmayer and Rozenberg (1979). The name is derived as follows. A *map OL-system* is a parallel rewriting system which operates on maps and does not allow for interaction between regions. In other words, regions are modified irrespective of what happens to other neighboring regions (a *context-free* mechanism). The system is *binary* because that a region can split into at most two daughter regions. It is *propagating* in the sense that the edges cannot be erased, thus regions (cells) cannot fuse or die. The *markers* represent a technique for specifying the positions of inserted edges that split the regions.

---

<sup>1</sup>The one-vertex case occurs when an edge forms a loop.

The choice of mBPMOL-systems as a modeling tool has two justifications. First, they are more powerful than other interactionless map rewriting systems described in the literature [de Boer 1989, de Boer 1987, Culik 1979]. In addition, markers have a biological counterpart in preprophase bands of microtubules, which coincide with the attachment sites for division walls formed during mitosis [Gunning 1981].

### 2.3 Definition and Operation of mBPMOL-systems

An mBPMOL-system  $\mathcal{G}$  is defined by specifying a finite alphabet of *edge labels*  $\Sigma$ , a *starting map*  $\omega$  with labels from  $\Sigma$ , and a finite set of *edge productions*  $P$ . In general, the edges are *directed*, which is indicated by a left or right arrow placed above the edge symbol. In some cases, the edge direction has no effect on the system operation. Such an edge is called *neutral* and no arrow is placed above the symbol denoting it. Each production is of the form  $A \rightarrow \alpha$ , where the directed or neutral edge  $A \in \Sigma$  is called the *predecessor*, and the string  $\alpha$ , composed of symbols from  $\Sigma$  and special symbols  $[, ], +, -$ , is called the *successor*. The sequence of symbols outside the square brackets specifies the edge subdivision pattern. Arrows can be placed above edge symbols to indicate whether the successor edges have directions consistent with, or opposite to, the predecessor edge. Pairs of matching brackets  $[$  and  $]$  delimit *markers*, which specify possible attachment sites for region-dividing walls. The markers are viewed as short branches which can be connected to form a complete wall. The strings inside brackets consist of two symbols. The first symbol is either  $+$  or  $-$ , indicating whether the marker is placed to the left or to the right of the predecessor edge. The second symbol is the marker label, with or without an arrow. The left arrow indicates that the marker is directed towards the predecessor edge, and the right arrow indicates that the marker is oriented away from that edge. If no arrow is present, the marker is neutral.

For example, in the production  $\vec{A} \rightarrow \vec{D}\overleftarrow{C}[-\vec{E}]\vec{B}F$ , the directed predecessor  $A$  splits into four edges  $D$ ,  $C$ ,  $B$  and  $F$ , and produces a marker  $E$  (Figure 1a). Successor edges  $D$  and  $B$  have the same direction as  $A$ , edge  $C$  has the opposite direction, and  $F$  is neutral. Marker  $E$  is placed to the right of  $A$  and is directed towards  $A$ . Note that this same production could be written as  $\vec{A} \rightarrow \vec{F}\overleftarrow{B}[+\vec{E}]\overleftarrow{C}\vec{D}$  (Figure 1b). As an example of a production with a neutral predecessor, consider  $A \rightarrow \overleftarrow{B}[-\overleftarrow{B}]x[+\overleftarrow{B}]\overleftarrow{B}$ . In this case the result of production application does not depend on the assumed direction of the predecessor edge (Figure 1c).

A *derivation step* in an mBPMOL-system consists of two phases:

1. Each edge in the map is replaced by successor edges and markers using the corresponding edge production in  $P$ .
2. Each region is scanned for *matching markers*.

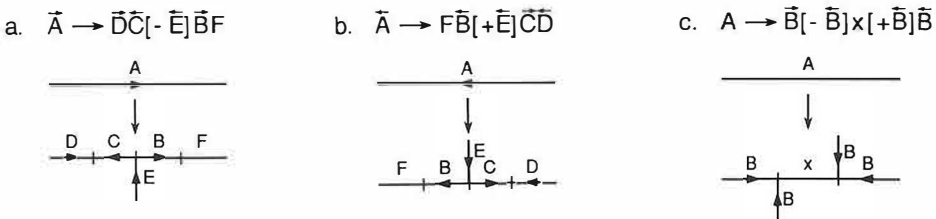


Figure 1: Examples of edge productions.

Two markers are considered matching if:

1. they appear in the same region,
2. they have the same label, and
3. one marker is directed away from its incident edge while the other is directed towards the edge, or both markers are neutral.

If a match is found, the markers are joined to create a new edge which will split the region. The search for matching markers ends with the first match found, even though other markers entering the same region may also form a match. From the user's perspective, the system behaves in a nondeterministic way since it autonomously chooses the pair of markers to be connected. The unused markers are discarded.

## 2.4 Examples of Map L-Systems

This section presents examples which illustrate the operation of mBPMOL-systems.

### L-system 1

$$\begin{aligned} \omega &: ABAB \\ p_1 &: A \rightarrow B[-A][+A]B \\ p_2 &: B \rightarrow A \end{aligned}$$

In L-system 1, production  $p_1$  creates markers responsible for region division, while production  $p_2$  introduces a delay, so that the regions are subdivided alternately by horizontal and vertical edges. The resulting sequence of maps is shown in Figure 2.

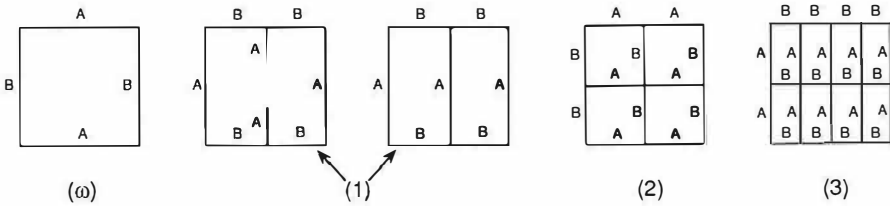


Figure 2: Developmental sequence defined by L-system 1. In the first step, a distinction is made between the edge rewriting phase and the connection of matching markers.

### L-system 2

$$\begin{aligned} \omega &: ABAB \\ p_1 &: A \rightarrow B[-A]x[+A]B \\ p_2 &: B \rightarrow A \end{aligned}$$

L-system 2 is a modified version of L-system 1. The only difference is the addition of an edge  $x$  which separates the markers in the successor of production  $p_1$ . This edge creates a Z-shaped offset between the inserted edges A (Figure 3). Z-offsets and symmetric S-offsets (Figure 4) can be observed in many biological structures [Lück 1988].

### L-system 3

$$\begin{aligned} \omega &: \overrightarrow{A} \overrightarrow{B} \overrightarrow{C} \overrightarrow{D} \\ p_1 &: \overrightarrow{A} \dashrightarrow \overrightarrow{D} [- \overrightarrow{A}] \overrightarrow{B} \\ p_2 &: \overrightarrow{B} \dashrightarrow \overrightarrow{B} \\ p_3 &: \overrightarrow{C} \dashrightarrow \overrightarrow{B} [- \overrightarrow{A}] \overrightarrow{B} \\ p_4 &: \overrightarrow{D} \dashrightarrow \overrightarrow{C} \end{aligned}$$

L-system 3 illustrates the operation of an mBPM0L-system with directed edges. Productions  $p_1$  and  $p_3$  create markers. Production  $p_4$  transforms edge D into C, so that in each derivation step there is a pair of edges A and C to which productions  $p_1$  and  $p_3$  apply. Production  $p_2$  indicates that edges B do not undergo further changes.<sup>2</sup> The resulting structure is that of a clockwise spiral (Figure 5).

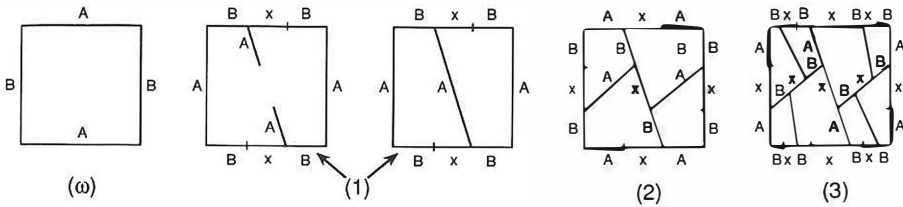


Figure 3: Developmental sequence defined by L-system 2.

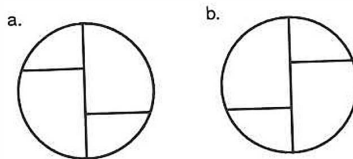


Figure 4: Offsets between four regions that result from the division of two regions sharing a common wall: (a) Z-offset, (b) S-offset.

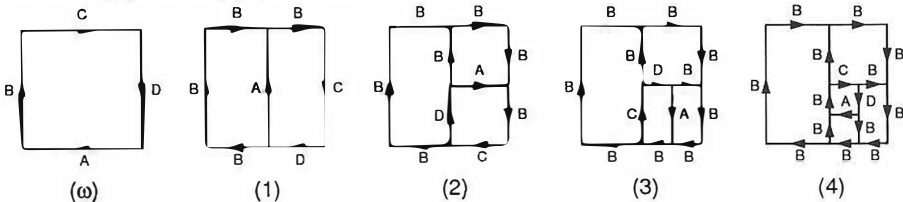


Figure 5: Developmental sequence defined by L-system 3.

<sup>2</sup>In further L-systems such identity productions are omitted.

### 3 GRAPHICAL INTERPRETATION OF MAP L-SYSTEMS

#### 3.1 Previous Work

Maps are graphs or topological objects without inherent geometric properties. In order to visualize them, some method for assigning geometric interpretation must be applied. In the scope of this paper, we are interested in the representation of cellular layers. Consequently, we will use the biologically-motivated terms, cell and wall, instead of their mathematical counterparts, region and edge.

Siero, Rozenberg and Lindenmayer (1982) proposed a method which, in the simplest case, is expressed by the following rules:

- walls are represented by straight lines,
- the starting map is represented by a regular polygon, bounded by the walls specified in the axiom,
- when a production subdivides a wall, all successor walls are of equal length, and
- the position of a wall resulting from the union of two matching markers is based on the position of these markers.

This *wall subdivision* method was used to draw Figures 2, 3 and 5. However, in the biological context it creates cells whose shapes are seldom observed in nature.

De Does and Lindenmayer (1983) proposed a *center of gravity* method which produces more realistic shapes. The main idea is to place each interior vertex of the map in the center of gravity of its neighbors. Such positioning of vertices has a sound biological justification: it minimizes hypothetical forces acting along cell walls [de Does 1983], thus bringing the entire structure to a state of minimum energy. However, if all vertices were positioned this way, the entire structure would collapse. In order to prevent this from happening, the vertices on the map perimeter are pushed outwards by a fixed distance. Unfortunately, this approach lacks biological justification and introduces sudden shape changes which make it unsuitable for animation purposes.

#### 3.2 The Dynamic Method

Assuming the dynamic point of view, the shape of cells and thus the shape of the entire organism results from the action of forces. The unbalanced forces due to cell divisions cause the gradual modification of cell shapes until an equilibrium is reached. At this point, new cell divisions occur, and expansion resumes.

The dynamic method is based on the following assumptions:

- the modeled organism forms a single cell layer,
- the layer is represented as a two-dimensional network of masses corresponding to cell corners, connected by springs which correspond to cell walls,
- the springs are always straight and adhere to Hooke's law,

- the cells exert pressure on their bounding walls; the pressure on a wall is directly proportional to the wall length and inverse proportional to the cell area,
- the pressure on a wall spreads evenly between the wall corners,
- the motion of masses is damped,
- other forces (for example, due to friction or gravity) are not considered.

The position of each vertex, and thus the shape of the layer, is computed as follows. As long as an equilibrium is not reached, unbalanced forces put masses in motion. The total force  $\vec{F}_T$  acting on a vertex  $X$  is given by the formula:

$$\vec{F}_T = \sum_{w \in W} \vec{F}_w + \vec{F}_d,$$

where:

- $\vec{F}_w$  are forces contributed by the set  $W$  of walls  $w$  incident to  $X$ , and
- $\vec{F}_d = -b\vec{v}$  is a damping force, expressed as the product of a damping factor  $b$  and vertex velocity  $\vec{v}$ .

A wall  $w \in W$  contributes three forces acting on  $X$  (Figure 6). The *tension*  $\vec{F}_s$  acts along the wall, and its magnitude is determined by Hooke's law:

$$\vec{F}_s = -k(l - l_0)$$

where  $k$  is the spring constant,  $l$  is the current spring length, and  $l_0$  is the rest length. The remaining two forces,  $\vec{F}_L$  and  $\vec{F}_R$ , are due to the *pressure* exerted by the cells on the left side and on the right side of the wall. Each force acts in the direction perpendicular to the wall, and is distributed equally between its two incident vertices. The magnitude of the force  $\vec{F}_L$  exerted by the cell on the left side of the wall equals  $p_L \cdot l$ , where  $p_L$  is the internal cell pressure and  $l$  is the wall length. A similar formula describes the force  $\vec{F}_R$ . The pressure is assumed to be inversely proportional to the cell area:  $p \sim A^{-1}$ . This assumption corresponds to the equation describing osmotic pressure,  $p = SRT$ , where  $S$  is the concentration of the solute ( $n$  moles per volume  $V$  of the solution),  $R$  is the ideal gas constant, and  $T$  is the absolute temperature [Sears 1985, Webster 1967]. Assuming that the cell volume  $V$  is proportional to the area  $A$  captured by the two-dimensional model under consideration ( $V = Ah$ ), pressure can be expressed as

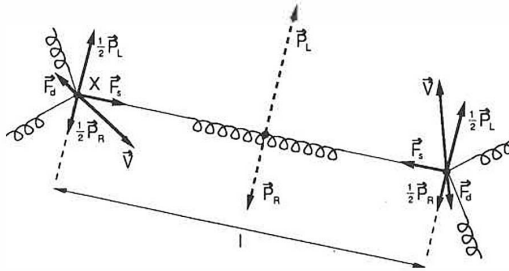


Figure 6: Forces acting on a cell corner  $X$  according to the dynamic method.

$$p = \frac{nRT}{Ah}.$$

Thus,  $p \sim A^{-1}$ , provided that the term  $nRT/h$  is constant.

A convenient formula for calculating the area  $A$  is:

$$A = \left| \sum_{i=1}^M (x_i - x_{i+1})(y_i + y_{i+1})/2 \right|$$

where  $(x_i, y_i)$  are coordinates of the  $M$  vertices surrounding region  $A$ ,  $x_{M+1} = x_1$ , and  $y_{M+1} = y_1$  [Bronshstein 1985].

The force  $\vec{F}_T$  acts on a mass placed at a map vertex. Newton's second law of motion applies:

$$m \frac{d^2 \vec{x}}{dt^2} = \vec{F}_T$$

where  $\vec{x}$  is the vertex position. Assuming that the entire structure has  $N$  vertices, we obtain a system of  $2N$  differential equations:

$$\begin{aligned} m_i \frac{d\vec{v}_i}{dt} &= \vec{F}_{T_i}(\vec{x}_1, \dots, \vec{x}_N, \vec{v}_i) \\ \frac{d\vec{x}_i}{dt} &= \vec{v}_i \end{aligned}$$

where  $i = 1, 2, \dots, N$ . The task is to find the sequence of positions  $\vec{x}_1, \dots, \vec{x}_N$  at given time intervals, assuming that the functions  $\vec{F}_{T_i}$  and the initial values of all variables:  $\vec{x}_1^0, \dots, \vec{x}_N^0$  and  $\vec{v}_1^0, \dots, \vec{v}_N^0$  are known. These initial values are determined as follows:

- Coordinates of the vertices of the starting map are included in the input data for the simulation.
- Positions of existing vertices are preserved through a derivation step. New vertices partition the divided walls into segments of equal length. The initial velocities of all vertices are set to zero.

The system of differential equations with the initial values given above represents an *initial value problem*. It can be solved numerically using the *forward (explicit) Euler method* [Fox 1987]. To this end, the differential equations are rewritten using finite increments  $\Delta \vec{v}_i$ ,  $\Delta \vec{x}_i$  and  $\Delta t$ :

$$\begin{aligned} \Delta \vec{v}_i^k &= \frac{1}{m_i} \vec{F}_{T_i}(\vec{x}_1^k, \dots, \vec{x}_N^k, \vec{v}_i^k) \Delta t \\ \Delta \vec{x}_i^k &= \vec{v}_i^k \Delta t \end{aligned}$$

where the superscripts  $k = 0, 1, 2, \dots$  indicate the progress of time,  $t = k\Delta t$ . The position and velocity of a point  $i$  after time increment  $\Delta t$  are expressed as follows:

$$\begin{aligned} \vec{v}_i^{k+1} &= \vec{v}_i^k + \Delta \vec{v}_i^k \\ \vec{x}_i^{k+1} &= \vec{x}_i^k + \Delta \vec{x}_i^k \end{aligned}$$

The iterative computation of the velocities  $\vec{v}_i^k$  and positions  $\vec{x}_i^k$  is carried out for consecutive values of index  $k$  until all increments  $\Delta \vec{v}_i$  and  $\Delta \vec{x}_i$  fall below a threshold value. This indicates that the equilibrium state has been approximated to the desired accuracy, and a derivation step can be performed. A system of equations corresponding to the new map topology is created, and

the search for an equilibrium state resumes. In such a way, the animation of a developmental process consists of periods of continuous cell expansion, delimited by instantaneous cell divisions. Continuity of cell shapes during divisions is preserved by the rule which sets the initial positions of vertices.

Color plate 1 illustrates the expansion of a structure generated by L-system 2. Plate 1a shows the structure immediately after the insertion of division walls. Plate 1b superimposes consecutive wall positions, with colors changing from blue to red as time progresses. Plate 1c describes the final structure at equilibrium. A smooth progression of shapes simulating the growth process can be easily observed.

## 4 A BIOLOGICAL EXAMPLE

In this section we apply the described simulation method to visualize the development of the fern gametophyte *Microsorium linguiforme*. Fern gametophytes represent the sexually reproducing life stage of fern plants. They show no differentiation into stem, leaf, and root, forming a plant body called a *thallus*. The development of a thallus can be conveniently described in terms of two types of activities: the activity of the *apical cell* giving rise to cell clones called *segments*, and the development of these segments. The modeling process captures repetitive patterns of cell divisions, so that large cellular structures can be described using a small number of productions.

### 4.1 Apical Activity

The apical cell is the originator of the gametophyte structure. It divides repetitively, giving rise each time to a new apical cell and a primary (initial) segment cell. The segment cells subsequently develop into multicellular segments. The division wall of an apical cell is attached to the thallus border on one side and to a previously created division wall on the other side. Thus, the division walls are oriented alternately to the left and to the right, yielding two columns of segments separated by a zig-zag dividing line (Figure 7). The recursive nature of the apical activity can be expressed by the following *cell production system*:

$$A_L \rightarrow S_L | A_R \quad A_R \rightarrow A_L | S_R$$

This notation means that the cell on the left side of the arrow sign produces two daughter cells separated by a wall.

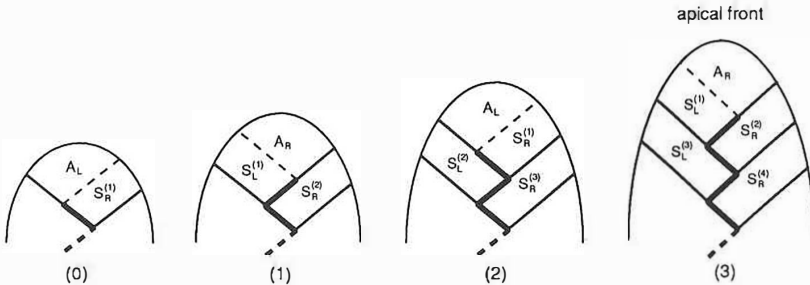


Figure 7: Apical production of segments. The labels  $A_R$  and  $A_L$  denote apical cells producing right segment  $S_R$  and left segment  $S_L$ , respectively. Dashed lines indicate the newly created division wall. The superscripts represent segment age. The internal structure of segments is not shown.

## 4.2 Division Pattern of Segments

In describing the structure of a segment, we distinguish between *periclinal* and *anticlinal* walls. Intuitively, periclinal walls are approximately parallel to the *apical front* of the thallus, and anticlinal walls are perpendicular to this front. A more formal definition is as follows:

- In a primary segment, the apical front wall and one or more walls opposing it are periclinal walls. The remaining walls are anticlinal walls.
- A division wall attached to the periclinal walls is an anticlinal wall, and vice-versa.

In *Microsorium*, a wall is never attached to a periclinal wall on one side and an anticlinal wall on the other side, so the above definition comprises all possible cases.

Microscopic observations of growing *Microsorium* gametophytes reveal that all segments follow the same developmental sequence, shown diagrammatically in Figure 8. The primary segment cell  $S_1$  is first divided by a periclinal wall into two cells,  $S_2$  and  $S_3$ . Subsequently, the basal cell  $S_3$  is divided by another periclinal wall into two “terminal” cells  $T$  which do not undergo further divisions. At the same time, the cell  $S_2$  lying on the thallus border is divided by an anticlinal wall into two cells of type  $S_1$ . Each of these cells divides in the same way as the primary cell. Consequently, the recursive nature of segment development can be captured by the following cell production system:

$$S_1 \rightarrow \frac{S_2}{S_3} \quad S_2 \rightarrow S_1 | S_1 \quad S_3 \rightarrow \frac{T}{T}$$

In the above rules, a horizontal bar denotes a periclinal wall between cells, and a vertical bar denotes an anticlinal wall.

## 4.3 The Development of the Entire Thallus

The development of the *Microsorium* thallus is a result of concurrent divisions of the apical and segment cells. A single division of the apical cell corresponds to a single step in the segment development. A developmental sequence which combines the activity of the apex and the segments is shown in Figure 9. This figure also reveals offsets between neighboring walls. On the basis of observation, it is assumed that periclinal division walls form S-offsets in the segments on the right side of the apex, and Z-offsets in the segments on the left side.

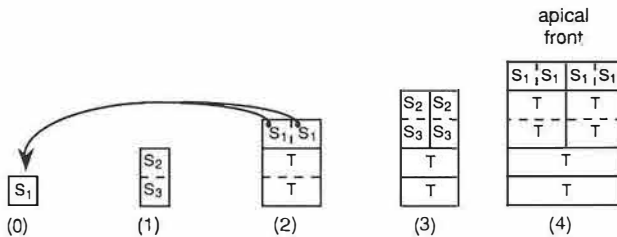


Figure 8: Developmental sequence of a *Microsorium* segment.



## L-system 4: Microsorium 1

$$\omega: \overline{A} \overline{D} \overline{x} \overline{b}$$

$$l_1: \overline{a} \rightarrow \overline{A} [+ \overline{b}] \overline{i}$$

$$l_2: \overline{b} \rightarrow \overline{e} [- \overline{B}] \overline{x} [+ \overline{h}] \overline{d}$$

$$l_3: \overline{d} \rightarrow \overline{f}$$

$$l_4: \overline{f} \rightarrow \overline{g} [- \overline{h}] \overline{x} [+ \overline{h}] \overline{d}$$

$$l_5: \overline{h} \rightarrow \overline{x} [- \overline{f}] \overline{x}$$

$$l_6: \overline{i} \rightarrow \overline{c}$$

$$l_7: \overline{c} \rightarrow \overline{i} [+ \overline{f}] \overline{i}$$

$$l_8: \overline{e} \rightarrow \overline{x} [+ \overline{x}] \overline{x}$$

$$l_9: \overline{g} \rightarrow \overline{x} [- \overline{x}] \overline{x} [+ \overline{x}] \overline{x}$$

$$r_1: \overline{A} \rightarrow \overline{a} [- \overline{B}] \overline{I}$$

$$r_2: \overline{B} \rightarrow \overline{E} [+ \overline{b}] \overline{x} [- \overline{H}] \overline{D}$$

$$r_3: \overline{D} \rightarrow \overline{F}$$

$$r_4: \overline{F} \rightarrow \overline{G} [+ \overline{H}] \overline{x} [- \overline{H}] \overline{D}$$

$$r_5: \overline{H} \rightarrow \overline{x} [+ \overline{F}] \overline{x}$$

$$r_6: \overline{I} \rightarrow \overline{C}$$

$$r_7: \overline{C} \rightarrow \overline{I} [- \overline{F}] \overline{I}$$

$$r_8: \overline{E} \rightarrow \overline{x} [- \overline{x}] \overline{x}$$

$$r_9: \overline{G} \rightarrow \overline{x} [+ \overline{x}] \overline{x} [- \overline{x}] \overline{x}$$

The apical cell divisions result from the application of productions  $r_1 - l_2$  (creation of a right segment) and  $l_1 - r_2$  (creation of a left segment). The subsequent segment cell divisions proceed in a symmetric way in right and left segments; we describe in detail the development of a right segment.

Concurrently with the insertion of wall segment B which creates segment  $S_R^{(1)}$ , wall D on the opposite side of the segment is transformed into F. This transformation introduces a one-step delay into the application of production  $r_4$  which, together with  $r_2$ , is responsible for the insertion of the first periclinal wall H into segment  $S_R^{(2)}$ . As the derivation progresses, production  $r_4$  inserts subsequent periclinal walls H between pairs of anticlinal walls F. Production  $r_3$  introduces a delay needed to create walls F which are inserted between periclinal walls H and apical walls I, using productions  $r_3$  and  $r_7$ . Production  $r_6$  plays a role analogous to  $r_3$  — it introduces a one-step delay into the cycle of creating markers F at the apical front of the segment. Thus, periclinal walls H and anticlinal walls F are produced alternately, in subsequent derivation steps. The last two productions,  $r_8$  and  $r_9$ , create terminal walls x which do not undergo further changes. The first such wall is inserted between walls labeled D and E during derivation step 3. Wall D separates segment  $S_R^{(2)}$  from  $S_L^{(1)}$ . Wall E lies on the border of the thallus. The subsequent walls x are inserted every second step between pairs of walls D; only production  $r_9$  is applied in these cases.

## 4.5 Including Basal Segments in the Model

L-system 4 was formulated under the assumption that all segments develop in the same way. However, in a real organism the first two segments, situated at the thallus base, form a modified pattern with less extensive cell divisions. The developmental sequence of a right basal segment is shown in Figure 10. The corresponding cell production system is given below.

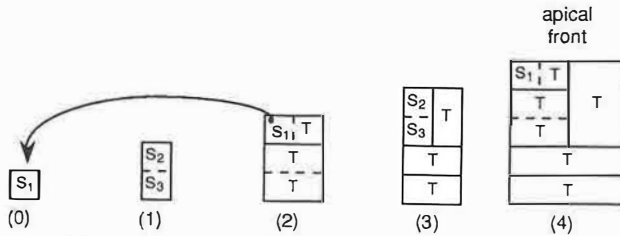


Figure 10: Developmental sequence of a basal *Microsorium* segment.

$$S_1 \rightarrow \frac{S_2}{S_3} \quad S_2 \rightarrow S_1 | T \quad S_3 \rightarrow \frac{T}{T}$$

The map L-system describing the development of a *Microsorium* gametophyte including basal segments has the following productions:

L-system 5: *Microsorium* 2

$$\begin{array}{ll} r_1 : \vec{A} \rightarrow \vec{a} [- \vec{B}] \vec{I} & r_9 : \vec{G} \rightarrow x [+ x] x [- x] x \\ r_2 : \vec{B} \rightarrow \vec{E} [+ \vec{b}] x [- \vec{H}] \vec{D} & r_{10} : \vec{J} \rightarrow \vec{L} \\ r_3 : \vec{D} \rightarrow [- \vec{m}] \vec{F} & r_{11} : \vec{K} \rightarrow \vec{N} \\ r_4 : \vec{F} \rightarrow \vec{G} [+ \vec{H}] x [- \vec{H}] \vec{D} & r_{12} : \vec{L} \rightarrow x [- \vec{M}] x \\ r_5 : \vec{H} \rightarrow x [+ \vec{F}] x & r_{13} : \vec{M} \rightarrow x [- \vec{L}] x \\ r_6 : \vec{I} \rightarrow \vec{C} & r_{14} : \vec{N} \rightarrow \vec{O} \\ r_7 : \vec{C} \rightarrow \vec{I} [- \vec{F}] \vec{I} & r_{15} : \vec{O} \rightarrow x [- \vec{L}] \vec{N} \\ r_8 : \vec{E} \rightarrow x [- x] x & \end{array}$$

Only productions describing the development of the right side of the thallus are given. Their predecessors are denoted by uppercase letters. The corresponding lowercase productions, which complete the L-system definition, can be obtained by switching the “case” of letters and the orientation of markers. The wall direction remains unchanged. For example, the right-side production

$$r_x : \vec{P} \rightarrow \vec{A} [- \vec{b}] \vec{C}$$

corresponds to the left-side production

$$l_x : \vec{p} \rightarrow \vec{a} [+ \vec{B}] \vec{c}$$

For more examples, see L-system 4.

A simulated developmental sequence generated by L-system 5 using the dynamic method to determine cell shape is given in Plate 2. Different colors are used to indicate the apical cell, the alternating “regular” segments, and the basal segments. A comparison of a developmental stage farther from the equilibrium (Plate 3) with a photograph of *Microsorium linguaeforme* (Plate 4) shows good correspondence between the model and reality with respect to structure topology, the relative sizes and shapes of cells, and the overall shape of the thallus.

## 5 CONCLUSIONS

This paper presented a modeling method for single-layered cellular structures, suitable for the animation of developmental processes. The topology is captured using mBPM0L-systems. The geometry results from a dynamic model that takes into account internal cell pressure and wall tension. The method is illustrated using a model of the gametophyte of *Microsorium linguaeforme*.

There are many possible refinements and extensions.

- The assumption that cell divisions occur after the structure has reached an equilibrium simplifies the computation, but is not essential to the modeling method. Cell divisions could also occur while the vertices are still in motion. In that case, velocities of existing vertices, as well as their positions, should be preserved.

- The described method is based on the assumption that cell divisions throw the structure out of an equilibrium state, and the subsequent process of reaching a new equilibrium describes the structure expansion. A physiological justification of this approach is an open problem.
- The assumption that wall strengths and solute concentrations defining osmotic pressure are the same for all walls and cells, and remain constant in time, may have to be relaxed for some structures.
- The method also assumes that cell states are not affected by the states of neighboring cells — the model is context-free. In some cases, cell interaction plays an important role in the control of development. To model this effect, a *context-sensitive* extension of map L-systems is needed.
- During the *cleavage* stage of embryo development, the structure consists of a single layer of cells which covers the surface of an imaginary sphere, called the *blastula* [Balinsky 1970]. By extending the method presented in this paper to a surface of a sphere, it was possible to model the development of worm and snail embryos [de Boer 1988]. For example, Plate 5 shows a ray-traced image of the embryo of *Patella vulgata*, modeled according to data in [van den Biggelaar 1977]. Nevertheless, both planar and spherical models operate on surfaces. Many cellular tissues and organs require truly three-dimensional models. A study of three-dimensional map systems, termed *cellworks*, was initiated in [Lindenmayer 1984]. Application of this theory to graphical simulation of development remains an open problem.

## ACKNOWLEDGEMENTS

We are deeply indebted to Professor Lindenmayer for inspiring discussions and comments on earlier versions of this paper. The reported research has been supported by an operating grant, equipment grants and a scholarship from the Natural Sciences and Engineering Research Council of Canada, and by an equipment donation from Apple Computer, Inc. Facilities of the Department of Computer Science, University of Regina, were also essential. All support is gratefully acknowledged.

## REFERENCES

- Balinsky BI (1970) *An introduction to embryology*. W. B. Saunders Co., Philadelphia, 3rd edition.
- Bronshtein S (1985) *Handbook of mathematics*. Van Nostrand, New York.
- Culik II K, Wood D (1979) A mathematical investigation of propagating graph 0L-systems. *Information and Control*, 43:50–82.
- de Boer MJM (1989) *Analysis and computer generation of division patterns in cell layers using developmental algorithms*. PhD thesis, Theoretical Biology Group, University of Utrecht, the Netherlands.
- de Boer MJM, Lindenmayer A, Fracchia FD (1988) Analysis and simulations of spiral cleavage patterns. Abstract in *European Journal of Cell Biology*, 47:18. Supplement 24.
- de Boer MJM, Lindenmayer A (1987) Map 0L-systems with edge label control: comparison of marker and cyclic systems. In H. Ehrig, M. Nagl, A. Rosenfeld, and G. Rozenberg, editors, *Graph-grammars and their application to computer science*, pages 378–392. Springer-Verlag. Lecture Notes in Comp. Sci. 291.

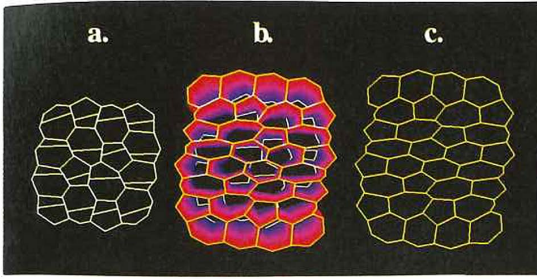


Plate 1: Layer expansion simulated using the dynamic method.

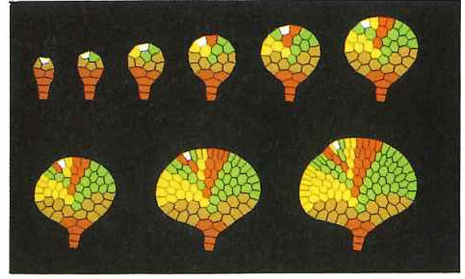


Plate 2: Simulated developmental sequence of *Microsorium linguaeforme*.

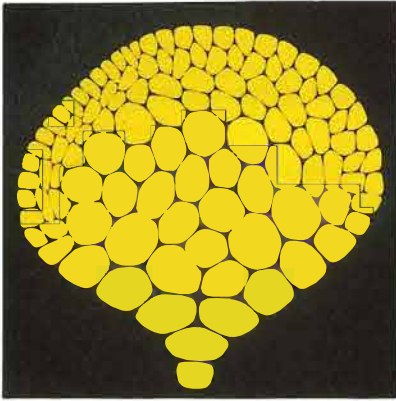


Plate 3: A model of *Microsorium linguae-forme*.

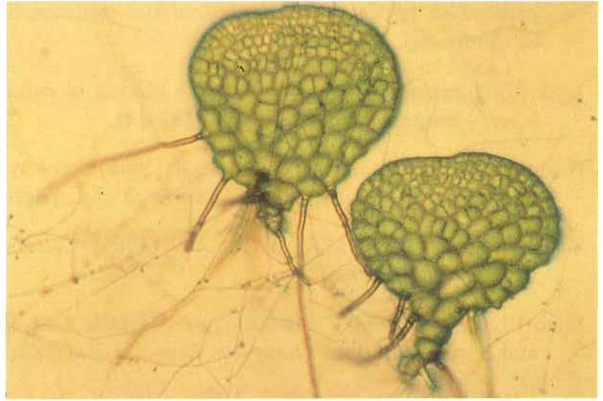


Plate 4: Photograph of *Microsorium linguae-forme* at magnification 60x.

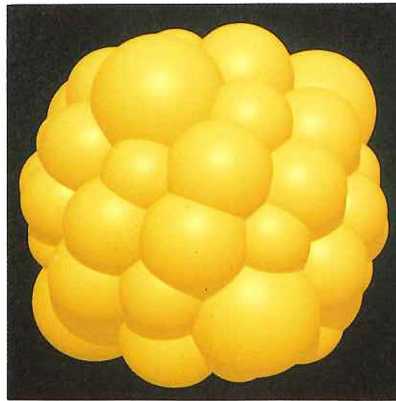


Plate 5: Ray-traced image of a modeled embryo of the snail *Patella vulgata*.

- de Does M, Lindenmayer A (1983) Algorithms for the generation and drawing of maps representing cell clones. In H. Ehrig, M. Nagl, and G. Rozenberg, editors, *Graph-grammars and their application to computer science*, pages 39–57. Springer-Verlag. Lecture Notes in Comp. Sci. 153.
- Fox L, Mayers DF (1987) *Numerical solution of ordinary differential equations*. Chapman and Hall, London.
- Gunning BES (1981) Microtubules and cytomorphogenesis in a developing organ: the root primordium of *Azolla pinnata*. In O. Kiermayer, editor, *Cytomorphogenesis in plants*, pages 301–325. Springer-Verlag, Wien. Cell Biology Monographs 8.
- Lindenmayer A (1984) Models for plant tissue development with cell division orientation regulated by preprophase bands of microtubules. *Differentiation*, 26:1–10.
- Lindenmayer A, Rozenberg G (1979) Parallel generation of maps: developmental systems for cell layers. In V. Claus, H. Ehrig, and G. Rozenberg, editors, *Graph-grammars and their application to computer science and biology*, pages 301–316. Springer-Verlag. Lecture Notes in Comp. Sci. 73.
- Lück JL, Lindenmayer A, Lück (1988) Models of cell tetrads and clones in meristematic cell layers. *Botanical Gazette*, 149(2):127–141.
- Nakamura A, Lindenmayer A, Aizawa K (1986) Some systems for map generation. In G. Rozenberg and A. Salomaa, editors, *The Book of L*, pages 323–332. Springer-Verlag, Berlin.
- Sears FW, Zemansky MW, Young HD (1985) *College physics*. Addison-Wesley Publ. Co., Reading, 6th edition.
- Siero PLJ, Rozenberg G, Lindenmayer A (1982) Cell division patterns: syntactical description and implementation. *Computer Graphics and Image Processing*, 18:329–346.
- Tutte WT (1982) *Graph theory*. Addison-Wesley Publ. Co., Reading.
- van den Biggelaar JAM (1977) Development of dorsoventral polarity and mesentoblast determination in *Patella vulgata*. *Journal of Morphology*, 154:157–186.
- Webster HC, Robertson DF (1967) *Medical and biological physics*. University of Queensland Press, Queensland.

**F. David Fracchia** received his B.Sc. from the University of Regina, Canada, in 1986 and a M.Math degree from the University of Waterloo, Canada, in 1988. He is currently pursuing a Ph.D. degree at the University of Regina. His research interests lie in the area of computer graphics, specifically the modeling of natural phenomena, scientific visualization, and physically-based modeling. Mr. Fracchia is a member of the ACM.

Address: Dept. of Computer Science, University of Regina, Regina, Saskatchewan, Canada S4S 0A2

**Przemyslaw Prusinkiewicz** is an associate professor of Computer Science at the University of Regina, Canada. His research interests include computer graphics, interactive techniques, and computer music. Dr. Prusinkiewicz received his M.S. in 1974 and Ph.D. in 1978, both in computer science, from the Technical University of Warsaw. He is a member of the ACM and IEEE CS.

Address: Dept. of Computer Science, University of Regina, Regina, Saskatchewan, Canada S4S 0A2

**Martin J. M. de Boer** received his B.Sc. in Biology in 1979, and M.S. in Mathematical Biology in 1984, both from the University of Amsterdam. From 1985 to 1989, he worked with Prof. Lindenmayer as a research assistant with the Theoretical Biology Group at the University of Utrecht, The Netherlands. He received his Ph.D. from the University of Utrecht in 1989.

Address: Theoretical Biology Group, University of Utrecht, Padualaan 8, Utrecht 3584 CH, The Netherlands